International Journal of Pure and Applied Mathematics
Volume 119 No. 17 2018, 1653-1667
ISSN: 1314-3395 (on-line version)
url: http://www.acadpubl.eu/hub/
Special Issue

http://www.acadpubl.eu/hub/

Non-similar solution of steady flow of an Eyring-Powell fluid with MHD effect: a vertical porous plate

M. Sudhakar Reddy*, L. Nagaraja

[1]Dept. of Mathematics, Madanapalle Institute of Technology and Science, A.P., 517325

*Corresponding author e-mail: msreddy.hod@gmail.com

Abstract

The present article is non-similar solution of steady flow an Eyring-Powell fluid with magnetohydrodynamic effect past a vertical porous medium. The transformed conservations solved numerically subject to the boundary conditions through the finite difference Keller-Box scheme. The behavior of velocity, temperature distributions corresponding to numerous physical parameters, Prandtl number, Darcy parameter, Eyring-Powell fluid Parameter, the local non-Newtonian parameter and magnetic parameter are graphically analyzed. Further, Skin friction, heat transfer rate is displayed in tabular forms.

Key words: *non-similar solution, Eyring-Powell fluid, MHD, Vertical porous plate*

Nomenclature

C_f	skin friction coefficient
f	non-dimensional stream function
Gr	grashof number
g	acceleration due to gravity
k	thermal conductivity of the fluid
Nu	the local nusselt number
Pr	prandtl number
T	temperature of the fluid
u, v	non-dimensional velocity components along the x- and y- directions, respectively
V	velocity vector x stream wise coordinate y transverse coordinate

Greek symbols

α	thermal diffusivity
β	fluid parameter

δ local non-Newtonian parameter
η dimensionless radial coordinate
μ dynamic viscosity
ν kinematic viscosity
θ dimensionless temperature
ρ density of non-Newtonian fluid
ξ dimensionless tangential coordinate
ψ dimensionless stream function
ε fluid parameter

Subscripts

w condition at the wall
∞ free stream condition

1. Introduction

The fluids which do not obey Newton's law of viscosity are called non-Newtonian fluids. The flow of non-Newtonian fluid has attained a great success in the theory of fluid mechanics due to its applications in biological sciences and industry. A few applications of non-Newtonian fluids are food mixing and chyme moment in the intestine, polymer solutions, paints, flow of blood, flow of nuclear slurries, flow of liquid metals and alloys, flow of mercury amalgams and lubrications with heavy oils and greases. Some important studies of different non-Newtonian fluids studied by [1-9].

Heat transfer has also prepared extensive interest due to its importance in industrial and environmental technologies with energy storage, gas turbines, nuclear plants, rocket propulsion, geothermal reservation, photovoltaic panels etc. The boundary conditions have also attracted some interest and this usually is a simulation in the wall thermal boundary condition. Recently, Swapna et al. [10] studied convective wall heating effects on hydro magnetic flow of a micropolar fluid. Hayat et al. [11] presented a simple isothermal nanofluid flow model through a porous space of homogeneous, heterogeneous reactions under the physically acceptable convective type boundary conditions. Junaid et al. [12] considered the three dimensional rotating flow of nanofluid induced by a convectively heated deformable surface. They used the shooting approach combined with fifth order Range- Kutta method to determine the velocity and temperature distributions above the sheet. Makinde et al. [13] studied the buoyancy effects on thermal boundary layer over a vertical plate subject to convective surface boundary conditions. Further analysis includes Aziz et al. [14]. Gupta et al. [15] used a variation finite element to simulate mixed convective radiative micropolar shrinking sheet flow with convective boundary conditions. Reddy et al. [16] presented convective boundary layer flow and heat transfer in an Eyring-Powell fluid past a horizontal circular cylinder in the porous medium. Ishak [17] discussed the similarity solutions for flow and heat transfer over a permeable surface with convective boundary conditions. Aziz [18-19] provided a similarity solution for laminar thermal boundary layer over the flat with convective boundary conditions and thermal slip. Beg et al. [20] analyzed Biot number and buoyancy effects on magnetohydrodynamic thermal slip flow. Subhashini et al. [21] studied wall transpiration and cross diffusion effects on free convective

boundary layers with convective boundary conditions. Mustafa et al. [22] addressed the rotating flow of nanofluids included by exponentially stretching sheet. They omplemented the convective boundary conditions to inspect the thermal boundary layer. Junaid et al. [23] theoretically studied the boundary layer flow of nanofluid past an exponentially stretching sheet.

The present investigation, consider the magnetohydrodynamic flow of Eyring-Powell fluid flow from a vertical porous plate. A finite difference numerical solution is obtained for the transformed non-linear two-point boundary value problem subject to physical appropriate boundary conditions at the cylinder surface and in the free stream. the impact of emerging thermo physical parameters are presented graphically and in the tables. The validation with previous non-Newtonian studies is included. The present problem has to the authours knowledge not appeared thus for in the scientific literature.

2. Mathematical flow model

Consider two dimensional, stable, incompressible boundary layer flow of an Eyring-Powell fluid past a circular cylinder in non-darcy porous medium in the presence of magnetic field effect. The boundary layer approximations, the leading conservation equations of Eyring-Powell model [29] is given as

$$\frac{\partial u}{\partial x}+\frac{\partial v}{\partial y}=0 \tag{1}$$

$$u\frac{\partial u}{\partial x}+v\frac{\partial u}{\partial y}=\left(\nu+\frac{1}{\rho\beta c}\right)\frac{\partial^2 u}{\partial y^2}-\frac{1}{2\rho\beta c^3}\left(\frac{\partial u}{\partial y}\right)^2\frac{\partial^2 u}{\partial y^2}-\frac{\sigma B_0^2}{\rho}u+g\beta(T-T_\infty)-\frac{\nu}{K}u \tag{2}$$

$$u\frac{\partial T}{\partial x}+v\frac{\partial T}{\partial y}=\alpha\frac{\partial^2 T}{\partial y^2} \tag{3}$$

The boundary conditions are set at the circulation and the edge of the boundary layer system, corresponding as follows

$$\begin{aligned} &As \quad y=0 \ : \quad u=0, \quad v=0, \ T=0 \\ &At \quad y\to\infty : \quad u\to 0, \quad T\to T_\infty \end{aligned} \tag{4}$$

Where the stream function is given by

$$\psi=4\nu Gr^{1/4}\left(f(\xi,\eta)+\frac{1}{4}\xi\right) \tag{5}$$

The stream function ψ is defined by $u=\partial\psi/\partial y$ and $v=-\partial\psi/\partial x$. In order to write the governing equations and the boundary conditions in the dimensionless form, the following non-dimensional quantities are introduced

$$\begin{aligned} &\xi=\frac{V_0 x}{\nu}Gr^{-1/4}, \qquad \eta=\frac{y}{x}Gr^{1/4}, M=\frac{\sigma B_0^2 x^2}{\rho\nu Gr^{1/2}}, \ E=\frac{K}{x^2}, \ \theta=\frac{T-T_\infty}{T_W-T_\infty}, \\ &Gr=\frac{g\beta(T_W-T_\infty)x^3}{\nu^3}, \ \mathrm{Pr}=\frac{\nu}{\alpha}, \qquad \varepsilon=\frac{1}{\nu\beta\rho c}, \qquad \delta=\frac{\nu^2 Gr^{3/2}}{2c^2x^4} \end{aligned} \tag{6}$$

In view of non-dimensional parameters (6), Equations (1) -(3) reduce to the following coupled, nonlinear, dimensionless differential equations (partial) are:

$$(1+\varepsilon) f''' - 2f'^2 + (3f+\xi) f'' - \varepsilon\delta f''^2 f''' - (M+E) f' + \theta = \xi\left(f' \frac{\partial f'}{\partial \xi} - f'' \frac{\partial f}{\partial \xi} \right) \quad (7)$$

$$\frac{1}{\mathbf{Pr}} \theta'' + f\theta' = \xi\left(f' \frac{\partial \theta}{\partial \xi} - \theta' \frac{\partial f}{\partial \xi} \right) \quad (8)$$

The transformed dimensionless boundary conditions are:

$$\begin{aligned} &f = 0, \quad f' = 0, \quad \theta = 1, \quad At \ \ \eta = 0 \\ &f' \to 0, \quad \theta \to 0, \quad As \ \ \eta \to \infty \end{aligned} \quad (9)$$

The manufacturing design quantities of physical attention include the skin-friction factor and Nusselt number, are given by

$$C_f Gr^{-3/4} = (1+\varepsilon)\xi f''(0) - \frac{\delta}{3}\varepsilon\xi^3 (f''(\xi,0))^3 \quad (10)$$

$$\frac{Nu}{\sqrt[4]{Gr}} = -\theta'(0) \quad (11)$$

3. Numerical Solution

The coupled boundary layer equations in a (ξ,η) coordinate system remain strongly nonlinear. A numerical method, the implicit difference Keller-Box method, is therefore deployed to solve the boundary value problem defined by Ens. (7) -(8) with boundary conditions (9). This procedure has been labeled concisely in Cebeci and Bradshaw [24] and Keller [25]. It has been used recently in polymeric flow dynamics by Subba Rao *et al*. [26-28] for viscoelastic models. The key stages involved are as follows:

a) Decomposition of nth order partial differential equation system to n first order equations
b) Finite difference discretization
c) Quasilinearization of non-linear Keller algebraic equations
d) Block-tridiagonal elimination of linearized Keller algebraic equations

a). Decomposition of nth order partial differential equation system to *n* first order equations

Equations (10) -(11) subject to the boundary conditions (12) are first cast as a multiple system of first order differential equations. New dependent variables are introduced: $u(x,y) = f', v(x,y) = f'', t(x,y) = \theta'$ These denote the variables for velocity, temperature respectively. Now equations (10) -(11) are solved as a set of fifth order simultaneous differential equations:

$$f' = u \quad (15)$$

$$u' = v \quad (16)$$

$$s' = t \quad (17)$$

$$(1+\varepsilon)v' - 2u^2 + (3f+\xi)v - \varepsilon\delta v^2 v' - (M+E)u + s = \xi\left(u\frac{\partial u}{\partial \xi} - v\frac{\partial f}{\partial \xi} \right) \quad (18)$$

$$\frac{1}{\Pr}t' + (3f + \xi)t = \xi\left(u\frac{\partial s}{\partial \xi} - t\frac{\partial f}{\partial \xi}\right) \tag{19}$$

Where primes denote differentiation with respect to variable η in terms of the dependent variables, the boundary conditions assume the form:

$$\begin{aligned} &At\ \eta = 0 \quad : \quad f = 0, \quad f' = 0, \quad \theta = 1 \\ &As\ \eta \to \infty \quad : \quad f' \to 0 \quad \theta \to 0 \end{aligned} \tag{20}$$

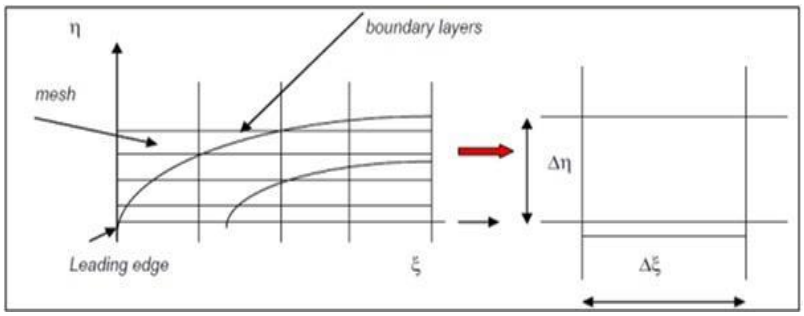

b). Finite difference discretization

A two dimensional computational grid is imposed on the ξ-η plane as depicted in Fig.1. The stepping process is defined by:

$$\eta_0 = \eta_{j-1} + h_j, \qquad j = 1,2,3,...,J, \eta_j = \eta_\infty \tag{21}$$

$$\xi^0 = 0, \quad \xi^n = \xi^{n-1} + k_n \qquad n = 1,2,3,...,N \tag{22}$$

$$g_{j-1/2}^{n-1/2} = \frac{1}{4}(g_j^n + g_{j-1}^n + g_j^{n-1} + g_{j-1}^{n-1}), \tag{23}$$

$$\left(\frac{\partial g}{\partial \eta}\right)_{j-1/2}^{n-1/2} = \frac{1}{2h_j}(g_j^n - g_{j-1}^n + g_j^{n-1} - g_{j-1}^{n-1}), \tag{24}$$

$$\left(\frac{\partial g}{\partial \xi}\right)_{j-1/2}^{n-1/2} = \frac{1}{2k^n}(g_j^n - g_{j-1}^n + g_j^{n-1} - g_{j-1}^{n-1}), \tag{25}$$

$$h_j^{-1}(f_j^n - f_{j-1}^n) = u_{j-1/2}^n \tag{26}$$

$$h_j^{-1}(u_j^n - u_{j-1}^n) = v_{j-1/2}^n \tag{27}$$

$$h_j^{-1}(s_j^n - s_{j-1}^n) = t_{j-1/2}^n \tag{28}$$

$$(1+\varepsilon)\left(v_j - v_{j-1}\right) - \frac{h_j(2+\alpha)}{4}\left(u_j + u_{j-1}\right)^2 + \frac{h_j(3+\alpha)}{4}\left(f_j + j_{j-1}\right)\left(v_j + v_{j-1}\right) + \frac{h_j}{2}\left(s_j + s_{j-1}\right)$$
$$+\frac{(3+\alpha)h_j}{2}v^{n-1}_{j-1/2}\left(f_j + f_{j-1}\right) - (M+E)\frac{h_j}{2}\left(u_j + u_{j-1}\right) - \frac{\varepsilon\delta}{4}\left(v_j - v_{j-1}\right)\left(v_j + v_{j-1}\right)^2 \quad (29)$$
$$-\frac{(3-\alpha)h_j}{2}f^{n-1}_{j-1/2}\left(v_j + v_{j-1}\right) + \frac{\xi h_j}{2}\left(v_j + v_{j-1}\right) = [R_1]^{n-1}_{j-1/2}$$

$$\frac{1}{\mathrm{Pr}}\left(t_j - t_{j-1}\right) + \frac{h_j(3+\alpha)}{4}\left(t_j + t_{j-1}\right)\left(f_j + f_{j-1}\right) + \frac{\xi h_j}{2}\left(t_j + t_{j-1}\right) - \frac{\alpha h_j}{4}\left(u_j + u_{j-1}\right)\left(s_j + s_{j-1}\right) + \frac{\alpha h_j}{2}t^{n-1}_{j-1/2} \quad (30)$$
$$\left(f_j + f_{j-1}\right) + \frac{\alpha h_j}{2}s^{n-1}_{j-1/2}\left(u_j + u_{j-1}\right) - \frac{\alpha h_j}{2}u^{n-1}_{j-1/2}\left(s_j + s_{j-1}\right) - \frac{\alpha h_j}{2}f^{n-1}_{j-1/2}\left(t_j + t_{j-1}\right) = [R_2]^{n-1}_{j-1/2}$$

$$\alpha = \frac{\xi^{n-1/2}}{k_n} \quad (31)$$

$$f^n_0 = u^n_0 = 0, \quad s^n_0 = 1, \qquad v^n_j = 0, \quad s^n_j = 0 \quad (32)$$

$$[R_1]^{n-1}_{j-1/2} = h_j\left(\begin{array}{l}(1+\varepsilon)(v')^{n-1}_{j-1/2} - (2-\alpha)(u^2)^{n-1}_{j-1/2} + (3-\alpha)f^{n-1}_{j-1/2}v^{n-1}_{j-1/2} - \varepsilon\delta(v^2)^{n-1}_{j-1/2}(v')^{n-1}_{j-1/2} \\ +\xi v^{n-1}_{j-1/2} + s^{n-1}_{j-1/2} - (M+E)u^{n-1}_{j-1/2}\end{array}\right) \quad (33)$$

$$[R_2]^{n-1}_{j-1/2} = h_j\left(\frac{1}{\mathrm{Pr}}(t')^{n-1}_{j-1/2} + \alpha u^{n-1}_{j-1/2}s^{n-1}_{j-1/2} + (3-\alpha)f^{n-1}_{j-1/2}t^{n-1}_{j-1/2} + \xi t^{n-1}_{j-1/2}\right) \quad (34)$$

The boundary conditions are:

$$f^n_0 = u^n_0 = 0, \quad s^n_0 = 1, \qquad v^n_j = 0, \quad s^n_j = 0 \quad (35)$$

c). Quasilinearization of non-linear Keller algebraic equations

Assuming $f^{n-1}_j, u^{n-1}_j, v^{n-1}_j, s^{n-1}_j, t^{n-1}_j$ to be known for $0 \le j \le J$, then equations (15)-(19) constitute a system of 5J+5 equations for the solutions of 5J+5 unknowns $f^n_j, u^n_j, v^n_j, s^n_j, t^n_j,\ j = 0, 1, 2, ..., J.$ This non-linear system of algebraic equations is linearized by means of Newtonian's method as explained by Keller, 1970[25].

d). Block-tridiagonal elimination solution of linear Keller algebraic equations

The linear system is solved by the block-elimination method, since it possesses a block-tridiagonal structure. The bock-tridiagonal structure generated consists of block matrices. The complete linear system is formulated as a block matrix system, where each element in the coefficient matrix is a matrix itself, and this system is solved using the efficient Keller-box method. The numerical results are strongly influenced by the number of mesh points in both directions. After some trials in the η-direction (radial coordinate) a larger number of mesh points are selected whereas in the ξ direction (tangential coordinate) significantly less mesh points are utilized. $\eta_{\max}$ has been set at 25 and this defines an adequately large value at which the prescribed boundary conditions are satisfied. ξ max is set at 3.0 for this flow domain. Mesh independence

is achieved in the present computations. The numerical algorithm is executed in **MATLAB** on a PC. The method demonstrates excellent stability, convergence and consistency, as elaborated by Keller, 1970[25].

4. Results & Discussion

The behavior of physical variables on the velocity f' and thermal fields θ is interpreted here. Figs.2–6 certifies the roles of dimensionless Eyring-Powell fluid parameters ε, local non-Newtonian parameter δ, Magnetic parameter M, Prandtl number $\Pr$ and Darcian parameter E. Where $\Pr = 0.71, \varepsilon = 0.1, \delta = 0.3, E = 0.1, M = 1.0$

The outline for velocity and temperature for various values of Prandtl number (Pr) as shown figure 2(a) and figure 2(b). It is observed that an increase in the Prandtl number significantly decelerates the flow i.e., velocity decreases. Also increasing Prandtl number is found to decelerate the temperature.

Figs. 3(a)–3(b) depict the response of velocity $f'(\eta)$, temperature $\theta(\eta)$ to a variation in the Darcy parameter E. The velocity is clearly enhanced considerably with increasing E as shown in Figs. 3a. The velocity peaks close to the plate surface are also found to be displaced further from the wall with increasing Darcy number. Decrease in temperature as shown in Figs. 3b, occurs with increasing E values.

Figures 4(a)-4(b) illustrates the effect of Eyring-Powell fluid parameter ε, on the velocity $f'(\eta)$ and temperature $\theta(\eta)$ distributions. Velocity is significantly decreased with increasing at larger distance from the cylinder surface owing to the simultaneous drop in dynamic viscosity. Conversely temperature is consistently enhanced with increasing values of ε.

Figures 5(a)-5(b) depict the velocity $f'(\eta)$ and temperature $\theta(\eta)$ distributions, with increasing local non-Newtonian parameter δ. Very little tangible effect is observed in fig. 5a, although there is a very slight decrease in velocity with increase in δ. Similarly there is only a very slight depression in temperature magnitudes in Fig. 5(b), with a rise in δ.

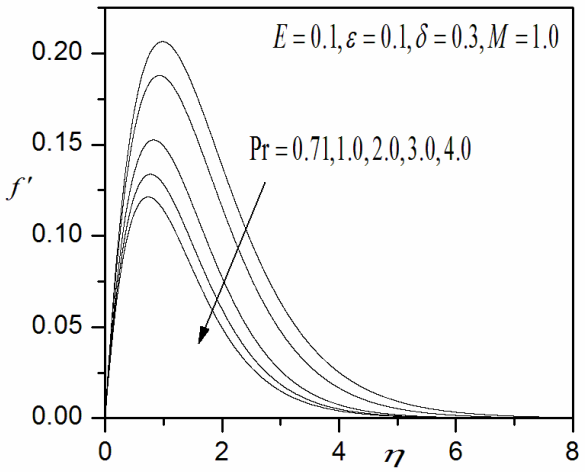

Fig. 2(a). Velocity field for different values of Pr

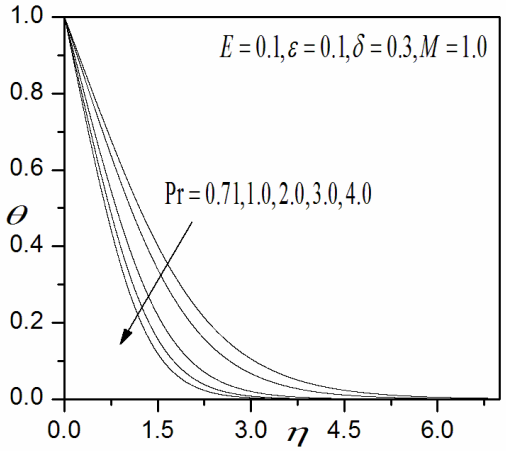

Fig. 2(b). Temperature field for different values of Pr

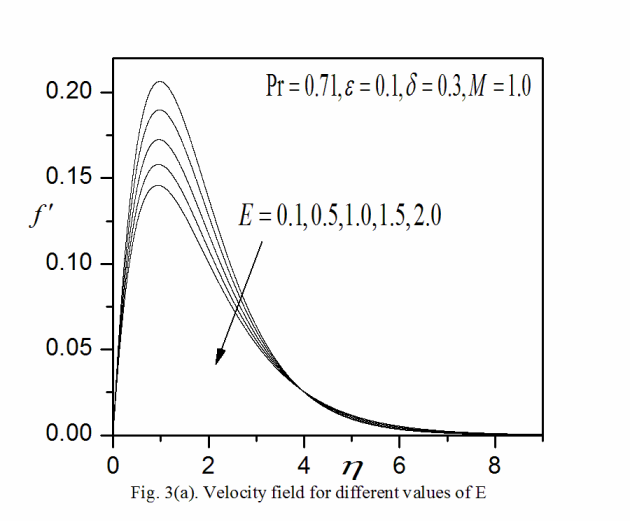

Fig. 3(a). Velocity field for different values of E

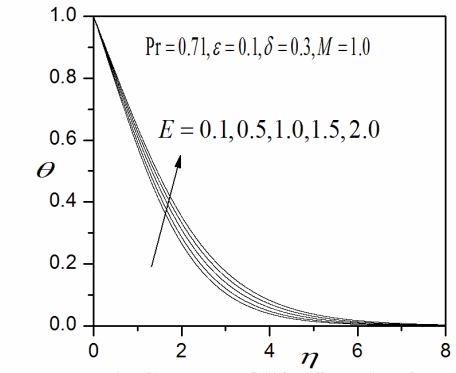

Fig. 3(b). Temperature field for different values of E

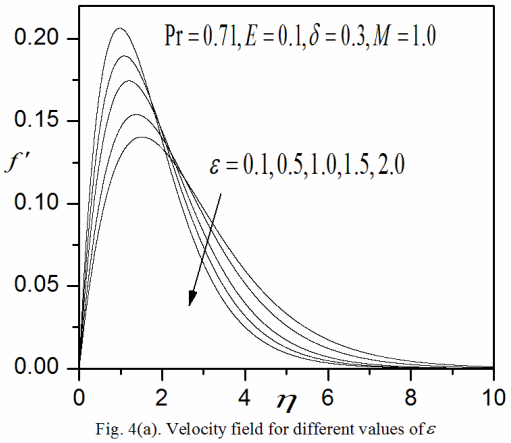

Fig. 4(a). Velocity field for different values of ε

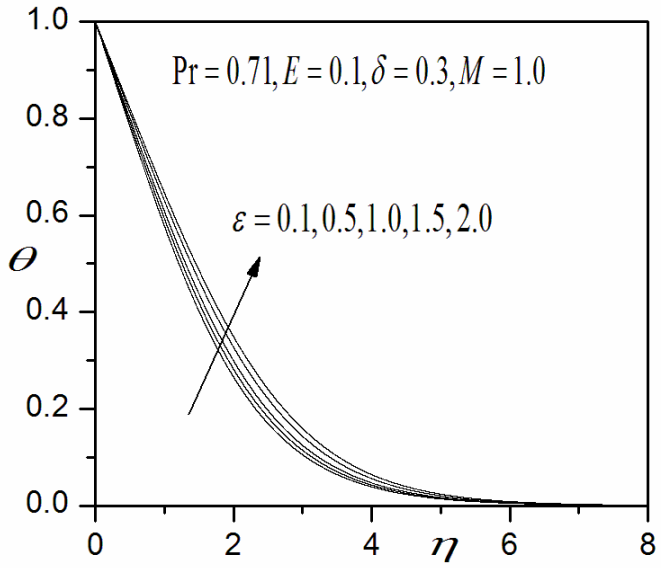

Fig. 4(b). Temperature field for different values of ε

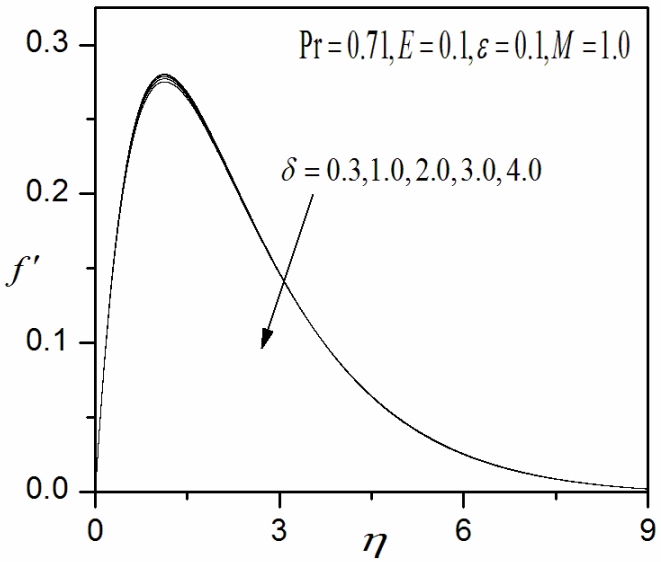

Fig. 5(a). velocity field for different values of δ

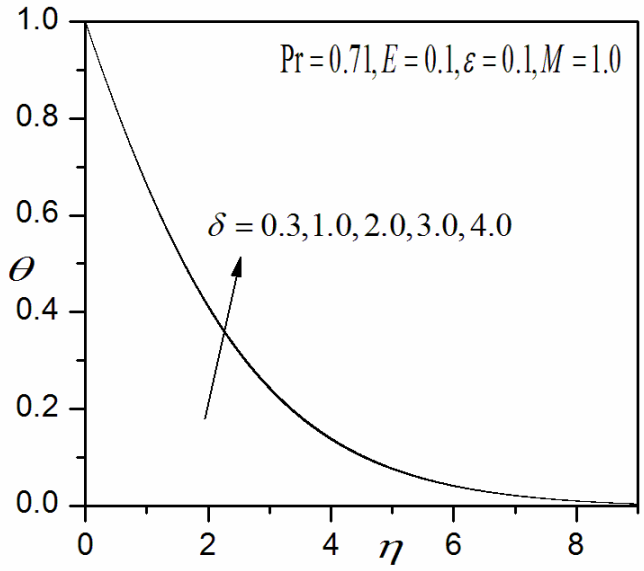

Fig. 5(b). temperature field for different values of δ

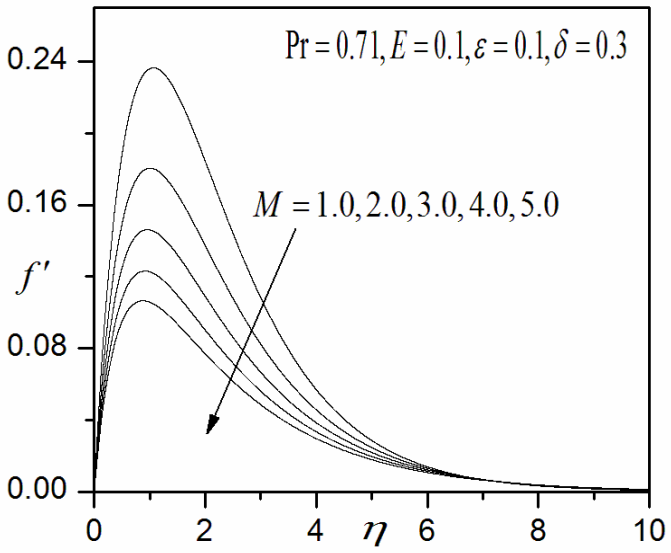

Fig. 6(a). velocity field for different values of M

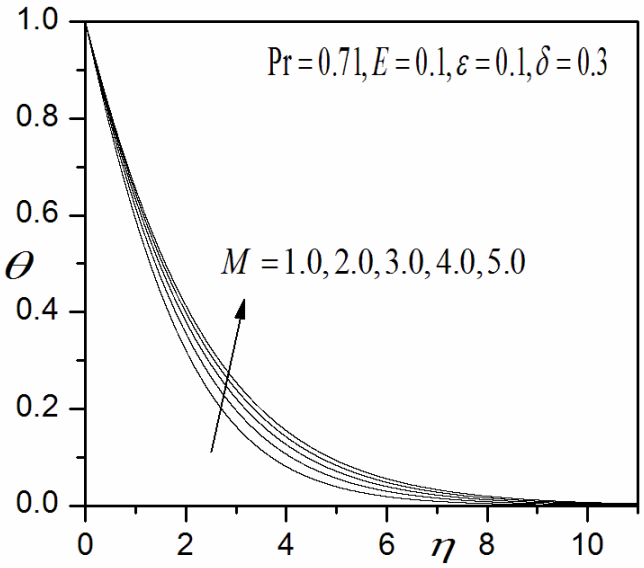

Fig. 6(b). temperature field for different values of M

Pr	O. Beg et.al(30)		Present results	
	Cf	*Nu*	*Cf*	*Nu*
0.5	1.2598	0.2184	1.2596	0.2186
0.7	1.1098	0.2810	1.1098	0.2808
1.0	1.1718	0.5101	1.1719	0.5105
2.0	0.7641	0.9396	0.7638	0.9391
3.0	0.5353	1.3392	0.5350	1.3396
5.0	0.3212	2.3163	0.3215	2.3160
7.0	0.2268	3.2426	0.2270	3.2429
8.0	0.1969	3.7064	0.1972	3.7050
10.0	0.1543	4.6360	0.1542	4.6364

Table: Comparison table for different values of Pr

Figures 6(a)-6(b) the dimensionless velocity $f'(\eta)$ and temperature $\theta(\eta)$ for various values of magnetic parameter M are shown. Fig. 6(a) represents the velocity profile for the different values of magnetic field parameter M . It is observed that velocity of the flow decreases throughout the fluid domain with increasing values of magnetic parameter M . Application of a magnetic field to an electrically conducting fluid produces a kind of drag-like force called Lorentz force. In Fig. 6(b), the temperature distribution increases with increasing magnetic values. The effect of Lorentz force on velocity profiles generated a kind of friction on the flow this friction in turns generated more heat energy which eventually increases the temperature distribution.

5. Conclusions

Numerical solutions have been presented for the buoyancy-driven flow and heat transfer of Eyring-Powell fluid flow external to a vertical porous plate. The Keller-box implicit second order accurate finite difference numerical scheme has been utilized to efficiently solve the transformed, dimensionless velocity and thermal boundary layer equations, subject to realistic boundary conditions. The computations have shown that:

- Increase the Prandtl number Pr decreases the velocity and temperature throughout the boundary layer.
- Increase the Eyring-Powell fluid parameter decreases the velocity and temperature near the boundary layer.
- Increasing the magnetic parameter decreases the velocity and temperature is increases through boundary layer regime.

References

1. J.E Dumn, K.R. Rajagopal, Fluids of differential type: critical review and thermodynamic analysis. *International Journal of Engineering Science* **33**: 689, (1995).
2. M. Patel, M.G. Timol, The stress-strain relationship for visco-inelastic non-Newtonian fluids. *International Journal Applied Math Mech* **6**: 79, (2010)
3. JN Kapur, BS. Bhatt, Sacheti NC. Non-Newtonian fluid flows. Meerut, India: *Pragati Prakashan* (1982).
4. C. Fetecau, C. Fetecau, Starting solutions for some unsteady unidirectional flows of a second grade fluid. *International Journal Engineering Science* **43**: 781(2005).
5. Akbar Noreen Sher, S. Nadeem, Numerical study of Williamson Nano-fluid flow in an asymmetric channel. *Results in Physics*, 3: 161(2013).
6. Akbar Noreen Sher, S. Nadeem, Thermal and velocity slip effects on the peristaltic flow of a six constant Jeffrey's fluid model. *International Journal Heat and Mass Transfer*, **55**: 3964(2012).
7. R. Ellahi, Effects of the slip boundary condition on non-Newtonian flows in a channel. *Commun Nonlinear Sci Nume Simul* **14**: 1377(2009).
8. S. Nadeem, RU. Haq, C. Lee., MHD flow of a Casson fluid over an exponentially shrinking sheet. *Sci Iran*, **19**: 1550(2012).
9. M. Qasim. Heat and mass transfer in a Jeffrey fluid over a stretching sheet with heat source/sink. *Alexandria Engineering Journal*, **52(4)**:571(2013).
10. G. Swapna, L. Kumar, O. Anwar Bég, B. Singh, Finite element analysis of radiative mixed convection magneto-micropolar flow in a Darcian porous medium with variable viscosity and convective surface condition. *Heat Transfer Asian Research*, **44(6)**: 515–532(2015).
11. T. Hayat, Z. Hussain, A. Alsaedi, M. Mustafa, Nanofluid flow through a porous space with convective conditions and heterogeneous-homogeneous reactions. *J Taiwan Inst Chem Eng* **70**:119–126(2017).
12. JA. Khan, M. Mustafa, A. Mushtaq, on three-dimensional flow of nanofluids past a convectively heated deformable surface: A numerical study. *International Journal Mass Transfer*, **94**:49–55(2016).
13. OD. Makinde, PO. Olanrewaju, Buoyancy effects on thermal boundary layer over a vertical plate with a convective surface boundary condition. *Trans ASME J Fluids Eng* **132(4)**:044502(2010).
14. OD. Makinde, A. Aziz, MHD mixed convection from a vertical plate embedded in a porous medium with a convective boundary condition. *Int J Therm Sci* **49(9)**:1813–1820(2010).
15. D. Gupta, L. Kumar, O. Anwar Beg, B. Singh, Finite element simulation of mixed convection flow of micropolar fluid over a shrinking sheet with thermal radiation. *Proc I Mech E Part E J Process Mech Eng*, 228**(1)** (2014). doi:10.1177/0954408912474586

16. L. Nagaraja, A. Subba rao, M. Sudhakar reddy, M. Surya Narayana reddy, Convection boundary layer flow and heat transfer in An eyring - powell fluid past a horizontal circular Cylinder in porous medium, *i-manager's Journal on Mathematics*, Vol. **6**. No. 1 (2017).
17. A. Ishak , Similarity solutions for flow and heat transfer over a permeable surface with convective boundary condition. *Appl Math Comput* **217(2)**:837–842(2010).
18. A. Aziz, A similarity solution for laminar thermal boundary layer over a flat plate with a convective surface boundary condition. *Commun Nonlinear Sci Numer Simul* **14(4)**:1064–1068(2009)
19. A. Aziz, Hydrodynamic and thermal slip flow boundary layers over a flat plate with constant heat flux boundary condition. *Commun Nonlinear Sci Numer Simul* **15(3)**:573–580(2010).
20. O. Anwar Bég, MJ. Uddin, M.M. Rashidi, N. Kavyani, Double-diffusive radiative magnetic mixed convective slip flow with Biot number and Richardson number effects. *J. Engineering Thermo physics* **23(2)**:79–97(2014).
21. SV. Subhashini, N. Samuel, I. Pop, Double-diffusive convection from a permeable vertical surface under convective boundary condition. *Int Commun Heat Mass Transf* **38(9)**:1183–1188(2011).
22. R. Ahmad, M. Mustafa, Model and comparative study for rotating flow of nanofluids due to convectively heated exponentially stretching sheet. *J Mol Liq* **220**:635–641(2016).
23. JA. Khan, M. Mustafa, T. Hayat, A. Alsaedi Numerical study on three-dimensional flow of nanofluid past a convectively heated exponentially stretching sheet. *Can J Phys* **93(10)**:1131–1137(2015).
24. T. Cebeci, P. Bradshaw, Physical and Computational Aspects of Convective Heat Transfer, *Springer*, New York (1984).
25. HB. Keller, A new difference method for parabolic problems, J. Bramble (Editor), Numerical Methods for Partial Differential Equations *Academic Press*, New York, USA(1970)
26. A. Subba Rao, VR. Prasad, N. Nagendra, KVN. Murthy, NB. Reddy and OA. Beg, Numerical Modeling of Non-Similar Mixed Convection Heat Transfer over a Stretching Surface with Slip Conditions. *World Journal of Mechanics* **5** 117-128 (2015)
27. V. Ramachandra Prasad, A. Subba Rao and O. Anwar Beg, Flow and Heat Transfer of Casson Fluid from a horizontal Circular Cylinder with Partial Slip in non-Darcy porous Medium, *Journal of Applied & Computational Mathematics*, **2**:3(2013).
28. V Ramachandra Prasad, A Subba Rao, N Bhaskar Reddy, B Vasu and O Anwar Be´g, Modelling laminar transport phenomena in a Casson rheological fluid from a horizontal circular cylinder with partial slip, J Process Mechanical Engineering 227(4) 309–326.
29. R. E. Powell, H. Eyring, Mechanism for relaxation theory of viscosity, Nature 7 (1944) 427-428, http://dx.doi.org/10. 1038/154427a0/
30. O.A Beg et. al, mathematical study of laminar boundary layer flow and heat transfer of a tangent hyperbolic fluid past a vertical porous plate with biot number effects, journal of applied fluid mechanics, 9(3), 2016